

1 **Green synthesis of silver and copper nanoparticles using ascorbic acid and**
2 **chitosan for antimicrobial applications**

3 **N. Mat Zain^{a,b}, A. G. F. Stapley^{a*}, G. Shama^a**

4 ^a**Department of Chemical Engineering, Loughborough University, Loughborough,**
5 **Leicestershire, LE11 3TU, United Kingdom.**

6 ^b**Department of Chemical Engineering, Universiti Malaysia Pahang, Highway Tun**
7 **Razak, 26300 Kuantan, Pahang, Malaysia.**

8 *Corresponding author: Tel: +44 (0)1509 222525, Fax: +44(0)1509 223923

9 Email addresses: shikin@ump.edu.my (N. Mat Zain), A.G.F.Stapley@Lboro.ac.uk,
10 G.Shama@Lboro.ac.uk

11

12 **Abstract**

13 Silver and copper nanoparticles were produced by chemical reduction of their
14 respective nitrates by ascorbic acid in the presence of chitosan using microwave
15 heating. Particle size was shown to increase by increasing the concentration of nitrate
16 and reducing the chitosan concentration. Surface zeta potentials were positive for all
17 nanoparticles produced and these varied from 27.8 to 33.8 mV. Antibacterial activities of
18 Ag, Cu, mixtures of Ag and Cu, and Ag/Cu bimetallic nanoparticles were tested using
19 *Bacillus subtilis* and *Escherichia coli*. Of the two, *B. subtilis* proved more susceptible
20 under all conditions investigated. Silver nanoparticles displayed higher activity than
21 copper nanoparticles and mixtures of nanoparticles of the same mean particle size.
22 However when compared on an equal concentration basis Cu nanoparticles proved
23 more lethal to the bacteria due to a higher surface area. The highest antibacterial
24 activity was obtained with bimetallic Ag/Cu nanoparticles with minimum inhibitory
25 concentrations (MIC) of 0.054 and 0.076 mg/L against *B. subtilis* and *E. coli*
26 respectively.

27

28 **Keywords: Bimetallic nanoparticles; Minimum inhibitory concentration; Minimum**
29 **bactericidal concentration; *Bacillus subtilis*; *Escherichia. coli***

30

31

32 **1. Introduction**

33 Interest in metal nanoparticles as antimicrobial agents is now over a decade old
34 (Dai & Bruening, 2002). The large number of particles that can be made and the high
35 surface area to volume ratio allows nanoparticles to be effective in very small amounts
36 (Sundaresan, Sivakumar, Vigneswaran, & Ramachandran, 2012). Ag nanoparticles
37 have been extensively used for biomedical applications (Marambio-Jones & Hoek,
38 2010). Cu is relatively non-toxic to mammals, (Flemming & Trevors, 1989) but is toxic
39 towards many micro-organisms and this offers new prospects for antimicrobial
40 treatments (Hsiao, Chen, Shieh, & Yeh, 2006).

41 A number of methods for producing Ag and Cu nanoparticles have been
42 developed using both physical and chemical approaches. The most frequently applied
43 method for the preparation of Ag nanoparticles is the chemical reduction of silver salt
44 solutions in water or an organic solvent to produce a colloidal suspension. The most
45 common approach for synthesizing Cu nanoparticles is by creating microemulsions
46 (Solanki, Sengupta, & Murthy, 2010). However, the microemulsion technique requires
47 large amounts of surfactants and organic solvents which increases the cost of
48 production (El-Nour, Eftaiha, Al-Warthan, & Ammar, 2010). Physical methods using
49 laser ablation, radiolysis or aerosol techniques, although effective, require expensive
50 instruments and consume large amounts of energy (Thakkar, Mhatre, & Parikh, 2010).
51 These methods typically makes use of agents which are both toxic and environmentally
52 polluting (Lim & Hudson, 2004).

53 Methods based on chemical reduction offer the best chance of being both low
54 cost and environmentally friendly. Ag nanoparticles have been synthesized using water
55 as solvent and starch as a capping agent and these were shown to have advantages
56 over conventional methods involving chemical agents that are associated with

57 environmental toxicity (Sharma, Yngard, & Lin, 2009). The synthesis of Ag
58 nanoparticles using chitosan as both a reducing and a capping agent has also been
59 developed (Sanpui, Murugadoss, Prasad, Ghosh, & Chattopadhyay, 2008). In addition,
60 Cu nanoparticles have been made using alginate as a stabilizing agent (Díaz-Visurraga
61 et al., 2012).

62 More recently, nanoparticles involving alloys of two metals have been produced.
63 Valodkar, Modi, Pal, & Thakore (2011) synthesized bimetallic Ag and Cu nanoparticles
64 using starch and Said-Galiev et al. (2011) have synthesized Ag and Cu nanoparticles
65 using chitosan. These had been treated with supercritical carbon dioxide followed by
66 reduction of Ag and Cu organometallic complexes with hydrogen to form metal–chitosan
67 nanoparticles. Bimetallic Ag and Cu nanoalloys have also been generated from silver
68 nitrate and copper acetate solution with hydrazine hydrate as a reducing agent (Taner,
69 Sayar, Yulug, & Suzer, 2011).

70 This work is an attempt to further develop the green synthesis of Ag and Cu
71 nanoparticles, mixtures of Ag and Cu nanoparticles (denoted as “Ag + Cu”) and alloy
72 nanoparticles of Ag and Cu (denoted as “Ag/Cu”) with chitosan as a stabilizing agent
73 and using microwave heating. The attraction of using chitosan for this function
74 compared to starch is that it possesses antimicrobial properties (No, Park, Lee, &
75 Meyers, 2002), and can be readily solubilised using organic acids (Muzzarelli et al.,
76 1984; Muzzarelli, 1985). Chitosan can form various chemical bonds with metals
77 components thus enhancing the stability of the nanoparticles (Muzzarelli, 2011). It has
78 low toxicity and it is therefore safe for human applications (Muzzarelli, 2010), although it
79 is acknowledged that the metallic nanoparticles produced may well have some
80 environmental toxicity (Li et al., 2010).

81 In this study nanoparticles were synthesized at different concentrations of
82 chitosan. The synthesized nanoparticles were characterized by spectrophotometry and
83 by the use of a zetasizer. Their antibacterial properties were tested using *Bacillus*
84 *subtilis* and *Escherichia coli*.

85

86 **2. Materials and methods**

87 **2.1 Reagents**

88 Copper (II) nitrate ($\text{Cu}(\text{NO}_3)_2 \cdot x\text{H}_2\text{O}$) (Sigma Aldrich Chemie GmbH, Steinheim,
89 Germany), silver nitrate (AgNO_3) (BDH Ltd, Poole, United Kingdom), L-ascorbic acid
90 (Sigma Aldrich, Poole, United Kingdom), acetic acid (Fisher Scientific, Loughborough,
91 United Kingdom) and chitosan (Sigma Aldrich, Poole, United Kingdom) were used for
92 synthesis of the nanoparticles. The molecular weight of the chitosan was in the range
93 50 000 - 190 000 Da and was 75-85% deacetylated. All reagents were used without
94 further purification.

95 **2.2 Preparation of chemical solutions**

96 The following solutions were all prepared using distilled water: silver nitrate (10,
97 30 and 50 mM), copper nitrate (10, 30 and 50 mM), ascorbic acid (10% w/v). Chitosan
98 solutions (1, 2 and 3% w/v) were prepared by dissolving chitosan in 1% (v/v) acetic acid
99 solution. These were then left for 3 days to allow the chitosan to completely dissolve
100 (Wei, Sun, Qian, Ye, & Ma, 2009).

101 **2.3 Preparation of nanoparticles**

102 **2.3.1 Ag and Cu nanoparticles**

103 For the preparation of Ag or Cu nanoparticles solution, 40 mL of silver nitrate or
104 copper nitrate solution (10, 30 or 50 mM) was mixed with 40 mL of chitosan solution (1,
105 2 or 3% w/v) and 4 mL of 10% (w/v) ascorbic acid solution. The reduction reaction was
106 carried out by heating in a microwave oven (EM-SI067 UK, Sanyo, China) at full power
107 of 800 W for 4 minutes (Valodkar, Modi, Pal, & Thakore, 2011).

108 **2.3.2 Bimetallic Ag/Cu nanoparticles**

109 For the preparation of bimetallic nanoparticles hereinafter referred to as "Ag/Cu"
110 nanoparticles, 20 mL of silver nitrate solution and 20 mL of copper nitrate solution were
111 mixed with 40 mL of 3% (w/v) chitosan and 4 mL of 10% (w/v) ascorbic acid solution.

112 The reaction was then carried out under microwave at full power of 800 W for 4 minutes
113 (Valodkar et al., 2011).

114 **2.3.3 Mixtures of Ag and Cu nanoparticles**

115 For the preparation of simple mixtures of Ag and Cu nanoparticles, subsequently
116 referred to as “Ag + Cu” nanoparticles, 40 mL of Ag nanoparticles and 40 mL of Cu
117 nanoparticles were separately synthesized in 3% (w/v) of chitosan as described in
118 section 2.3.1 and then mixed together (Valodkar et al., 2011).

119 **2.4 Characterization of nanoparticles**

120 **2.4.1 Spectrophotometry**

121 UV-vis absorption spectra of Ag, Cu, Ag/Cu and Ag + Cu nanoparticles solutions
122 were taken over the wavelength range 200 to 800 nm using UV-vis
123 spectrophotometer model UV mini-1240 (Shimadzu Corporation, Kyoto, Japan).

124 **2.4.2 Particle size and zeta potential analysis**

125 Particle sizes of Ag, Cu, Ag/Cu and Ag + Cu nanoparticle solutions were
126 measured using a Zetasizer instrument (Model ZEM5002, Malvern Instruments Ltd,
127 Malvern, UK) using UV Grade cuvettes after treatment in an ultrasonic water bath
128 (Model FB11012, Fisherbrand, Loughborough, UK) for 30 min to break up any
129 aggregates present (Ribeiro, Hussain, & Florence, 2005). The zeta potentials of each
130 type of nanoparticle were measured using a Zetasizer model 3000HS (Malvern
131 Instrument Ltd, Malvern, UK). All measurements were performed in triplicate.

132 **2.5 Microbiological methods**

133 **2.5.1 Bacteria**

134 The Gram-positive bacterium, *Bacillus subtilis* ATCC 6633 was obtained from the
135 National Collections of Industrial, Food and Marine Bacteria (NCIMB), Aberdeen,
136 Scotland and the Gram-negative bacterium, *E. coli* K12 was kindly donated by Dr Jon
137 Hobman of Nottingham University, Nottingham, United Kingdom.

138 **2.5.2 Cultivation of bacteria**

139 Bacteria were taken from frozen (-80 °C) stock and streaked onto Tryptone Soy
140 Agar (TSA) and incubated overnight at 37 °C. A single colony was then used to
141 inoculate 100 mL of Tryptone Soy Broth (TSB) in a 500 mL Erlenmeyer flask which was
142 then placed in a shaking incubator at 37 °C at a speed of 140 rpm for 12 hours.
143 Following this, 100µL of this culture was used to inoculate 100 mL of fresh TSB
144 incubated at the same conditions as described above until the mid-logarithmic phase
145 had been attained. The culture at this point was suitably diluted in phosphate buffered
146 saline (PBS) to yield a suspension containing 10⁸ colony forming units (CFU) per mL.
147 Identical procedures were followed for both *B. subtilis* and *E. coli*.

148 **2.5.3 Determination of the minimum inhibitory concentration (MIC) and minimum** 149 **bactericidal concentration (MBC)**

150 A range of dilutions of nanoparticles in sterile distilled water were prepared and 4
151 mL of the dilution was added to 20 mL of TSB medium with 20 mL of bacteria of 10⁸
152 CFU/mL and incubated in an incubator shaker (model CERTOMAT[®] BS-1, Sartorius,
153 Göttingen, Germany) at 37 °C overnight (Cao *et al.*, 2010). The MIC was determined by
154 visual observation and confirmed by turbidity measurement using a UV-vis
155 spectrophotometer (Jenway 6300, Bibby Scientific Ltd, Essex, UK) at 600 nm before
156 and after incubation. Diluted aliquots (100µL) of those samples in which growth of the
157 bacteria was not observed were spread plated using TSB to determine the minimum
158 bactericidal concentration (MBC). The samples were incubated at 37 °C overnight and
159 the colonies formed were observed. The MBC was determined as the lowest
160 concentration that inhibited the visible growth of the bacteria tested (Wei *et al.*, 2009).

161 **2.6 Statistical analysis**

162 The data from triplicate experiments are presented as the mean and the standard
163 error of the mean. The statistical analysis of the results was performed using one-way
164 ANOVA with Bonferroni multiple comparison post hoc test. All statistical analyses were
165 performed using IBM SPSS Statistics 21.0 (SPSS UK Ltd., Surrey, United Kingdom).

166

167 **3. Results and discussion**

168 **3.1 Physical characteristics**

169 Images of the nanoparticle suspensions prepared according to the methods
170 described above are presented in Fig. 1. The formation of colloidal suspensions of
171 nanoparticles was evident from visual inspection of the reagent mixtures following
172 microwave heating. Ag nanoparticles (Fig. 1a) were of a light yellow colour which
173 became stronger as the chitosan concentration was increased. The formation of metal
174 nanoparticles was confirmed by UV-vis spectrophotometry. Fig. 2a shows an
175 absorbance spectrum with a peak at approximately 420 nm, indicating the formation
176 of Ag nanoparticles (Ahmad et al., 2003). Ag nanoparticles have previously reported to
177 be of yellowish colour in aqueous solution (Perera et al., 2013). The colour and
178 absorbance spectra at 420 nm is due to the excitation of surface plasmon vibrations of
179 Ag atoms (Twu, Chen, & Shih, 2008). Increasing the chitosan concentration was found
180 to result in a slight downward shift in the peak absorbance coupled with an overall
181 increase in absorbance. These results are consistent with those obtained by Huang,
182 Yuan, & Yang (2004) who synthesized Ag nanoparticles in chitosan by reduction with
183 sodium borohydride.

184 The Cu nanoparticles (Fig. 1b), varied in colour from light pink to deep red as the
185 concentration of chitosan was increased. The UV spectrum (Fig. 2b) showed a peak at
186 550 nm, which confirms the presence of Cu nanoparticles. These have been reported to
187 be in the range of 500 to 600 nm (Mallick, Witcomb, & Scurrrell, 2006). Similarly, it has
188 been reported that the color of the freshly synthesized Cu nanoparticle stabilized using
189 a water soluble aminoclay matrix suspension was red which is characteristic of Cu
190 nanoparticles (Datta, Kulkarni, & Eswaramoorthy, 2010).

191 Fig. 1c shows that mixtures of Ag and Cu nanoparticles are orange in color (as
192 would be expected from a blend) but alloyed nanoparticles of Ag and Cu were dark
193 brown. Taner et al. (2011) formed bimetallic Ag/Cu nanoparticles by bringing about the

194 reduction of metal salts in aqueous solution with hydrazine hydrate and also reported
195 that the colour of the suspension was dark brown. UV-vis spectra of Ag + Cu and Ag/Cu
196 nanoparticles are presented in Fig. 2c. The Ag + Cu spectra show two distinct peaks at
197 420 and 550 nm, indicating a physical mixture of Ag and Cu nanoparticles. The Ag/Cu
198 nanoparticles, on the other hand, showed a single absorbance peak at an intermediate
199 ratio confirming that a bimetallic alloy had been formed (Valodkar et al., 2011).

200 In this study, chitosan was solubilized using dilute acetic acid solution. The
201 chitosan reacts with H^+ from the acid solution to produce protonized chitosan with $-NH_3^+$
202 functional groups. The introduction of these functional groups into the chitosan
203 backbone improves its solubility in water. When silver and copper nitrate were added to
204 the chitosan solution, Ag^+ and Cu^{2+} ions would attach to chitosan macromolecules by
205 electrostatic interactions, because the electron-rich oxygen atoms of polar hydroxyl and
206 ether groups of chitosan are likely to interact with electropositive metal cations. A
207 reducing agent is required to provide the free electrons needed to reduce ions and to
208 form nanoparticles (Tolaymat et al., 2010). In this study, ascorbic acid was used as the
209 reducing agent. Ag and Cu nanoparticles thus were formed by the reduction of Ag^+ and
210 Cu^{2+} ions respectively, with an excess of ascorbic acid (for 100% conversion). The Ag
211 and Cu nanoparticles are stabilized by protonized chitosan to prevent aggregation and
212 to control the size of final nanoparticles produced. The same mechanism applies for the
213 synthesis of Ag/Cu nanoparticles.

214 **3.2 Mean particle size**

215 The changes in UV-vis absorbance referred to above indicate that the size of
216 nanoparticles formed altered with the concentration of chitosan, which operates as a
217 controller of nucleation as well as a stabilizer (Huang et al., 2004). Fig. 3 shows the
218 mean particle size of Ag and Cu nanoparticles synthesized using 10 mM salt solution at
219 different concentrations of chitosan. It was observed that the mean particle sizes of both
220 Ag and Cu nanoparticles decreased with increasing chitosan concentration and that for
221 the same chitosan concentration Ag nanoparticles were slightly larger than Cu
222 nanoparticles as presented in Fig. 3. This decrease is due to a protective action by

223 chitosan whereby chitosan may prevent the growth of the nanoparticles by adsorbing
224 onto their surfaces (Esumi, Takei, & Yoshimura, 2003).

225 The effects of silver and copper nitrate concentration on the mean particle size of
226 the nanoparticles are presented in Fig. 4. As the concentration of silver and copper
227 nitrate increased from 10 to 50 mM, the size of nanoparticles increased almost
228 proportionately. At the same concentration of chitosan, with increased concentration of
229 metal salts, less protonized chitosan absorbed onto the pre-formed nanoparticles, and
230 therefore larger nanoparticles were formed (Leung, Wong, & Xie, 2010). Statistical
231 analysis showed that the mean particle sizes of the nanoparticles are significantly
232 different and influenced by the concentrations of chitosan and metal salts. Therefore,
233 the size of the nanoparticles may be controlled either by adjusting the concentration of
234 metal ions or the concentration of chitosan during the synthesis process.

235 **3.3 Zeta potential**

236 The zeta potential is a crucial parameter for determining the stability of
237 nanoparticle suspensions. For a physically stable nanoparticle suspension to be
238 stabilized solely by electrostatic repulsion, a zeta potential of ± 30 mV is required as a
239 minimum (Singare et al., 2010). The mutual repulsion of nanoparticles depends on
240 having either a large negative or positive zeta potential. Zeta potential measurements of
241 the nanoparticles are presented in Fig. 5. These show that Ag nanoparticles have a
242 positive surface charge which increases with chitosan concentration from +23.8 mV at
243 1% (w/v) to +32.1 mV at 3 % w/v chitosan solution. Cu nanoparticles had a slightly
244 higher positive surface charge which ranged from +26.4 mV at 1% (w/v) to +33.9 mV at
245 3% (w/v), although statistically the zeta potentials of Ag and Cu nanoparticles were not
246 found to be significantly different to each other. The zeta potential of the nanoparticles
247 increases with chitosan concentration due to the greater availability of protonized –
248 NH^{3+} on the surface of nanoparticles formed. This will produce a greater electrostatic
249 repulsion between the particles and therefore a lower incidence of agglomeration and
250 resulting in a more stable nanoparticle dispersion.

251 Fig. 5b shows zeta potentials of Ag, Cu, Ag + Cu and Ag/Cu nanoparticles
252 prepared from 50 mM metal salt solutions and 3% (w/v) chitosan solutions respectively.
253 In this instance the Ag nanoparticles have a slightly higher surface charge (+37.8 mV)
254 than Cu nanoparticles (+35.5 mV). Mixed (Ag + Cu) nanoparticles gave a value of +39.1
255 mV and Ag/Cu nanoparticles one of +35.2 mV. These differences were not statistically
256 significant.

257 As there may be an effect of particle size on the zeta potentials of the four
258 nanoparticle types (Ag, Cu, Ag + Cu and Ag/Cu), the zeta potentials were compared for
259 selected samples which most closely corresponded to a mean particle size of 200 nm.
260 These were synthesized in 3% (w/v) chitosan and corresponded to metal ion
261 concentrations of 12.1, 32.0 and 18.2 mM for Ag, Cu and Ag/Cu respectively. Ag + Cu
262 was made by mixing Ag prepared at 12.1 mM with Cu prepared at 32.0 mM. The
263 corresponding zeta potentials are +33.8, 33.1, 32.6 and 33.3 mV for Ag, Cu, Ag+Cu and
264 Ag/Cu respectively (Fig. 5c). These are very similar to those shown in Fig. 5b where all
265 samples were prepared with a 50 mM solution (corresponding to mean particle sizes of
266 793, 292, 542 and 633 nm respectively). This finding reveals that the concentration of
267 metal salts used in the preparation does not significantly affect the charge of the
268 nanoparticles. The results obtained here are consistent with those of Xiong et al. (2013),
269 in which it was reported that the zeta potential of Cu nanoparticles is +32 mV,
270 suggesting that that value was high enough to maintain stable colloidal dispersions.

271 **3.4 Antimicrobial properties**

272 MIC and MBC tests were performed to assess the antibacterial activity of the
273 nanoparticles towards *B. subtilis* and *E. coli*. The MIC is defined as the lowest
274 concentration at which there is no visible growth whilst MBC is defined as the lowest
275 concentration at which no colony is observed (Wei et al., 2009). MIC and MBC values
276 towards *B. subtilis* and *E. coli* of Ag, Cu, Ag/Cu and Ag + Cu nanoparticles prepared
277 from 50 mM metal salt solutions are shown in Table 1. A lower MIC or MBC
278 corresponds to higher antibacterial effectiveness. As a control, to assess the possible
279 antimicrobial action of ascorbic acid, separate experiments were performed in which
280 samples were prepared according to the method in Section 2.3.1, but in the absence of
281 chitosan and silver or copper nitrate and tested against both *E. coli* and *B. subtilis*.

282 These samples showed no bactericidal effect when undiluted, but an inhibitory effect at
283 full strength and 1/2 dilution. However, under such conditions the ascorbic levels are
284 typically a thousand times greater than those present in the nanoparticle suspensions
285 detailed in Table 1, and therefore any antimicrobial effects directly due to the presence
286 of ascorbic acid in our experiments can be neglected.

287 The results show that Ag nanoparticles have significantly higher MIC and MBC
288 values for *B. subtilis* and *E. coli* than Cu nanoparticles at the same concentration of
289 chitosan (3% w/v) and metal salts (50 mM). The results presented here demonstrated
290 that at the same metal salts concentration, Cu nanoparticles have a characteristically
291 smaller particle size than Ag nanoparticles. Smaller particle size tends to enhance
292 antibacterial properties because as size decreases, there are a larger number of atoms
293 on the surface available to interact with bacteria (Marambio-Jones & Hoek, 2010). A
294 mixture of Ag and Cu nanoparticles at 50 mM showed intermediate behaviour although
295 statistically this was similar to that of Ag nanoparticles for both type of bacteria. The 50
296 mM Ag/Cu alloy nanoparticles showed the highest antibacterial effectiveness of all.

297 All the nanoparticles showed very similar values for MIC and MBC which shows
298 that the nanoparticles have a bactericidal rather than bacteriostatic effect on these two
299 bacteria.

300 Valodkar *et al.*, 2011 reported MIC and MBC values of 0.26 and 0.78 mg/L for 10
301 mM Ag nanoparticles and the MIC and MBC of 0.23 and 0.65 mg/L for 10 mM Ag/Cu
302 alloy nanoparticles against lower bacterial concentrations (10^4 CFU/mL) of *E. coli* than
303 were employed here (10^8 CFU/mL). Taner *et al.*, 2011 reported an MIC value only of
304 >150 mg/L for Ag nanoparticles and identical values for MIC and MBC of Ag?Cu
305 nanoparticles of 0.5 mg/L against high concentrations (10^8 CFU/mL) of *E. coli*. The
306 MIC/MBC values reported here are lower than those achieved by Valodkar *et al.*, 2011
307 and Taner *et al.*, 2011 which indicated better antibacterial activity and suggested that
308 chitosan, which serves as stabilizing agent is also contributing to the antimicrobial
309 effect. The findings obtained here are not directly comparable with those of Said-Galiev
310 *et al.* (2011) as they did not report their findings in terms of MIC or MBC. Huang *et al.*,
311 (2004) synthesized nanoparticles using chitosan but did not report on the antimicrobial

312 activity of their nanoparticles. The findings reported here reveal that MIC/MBC values of
313 bimetallic alloy nanoparticles were substantially lower than that of pure i.e. single metal
314 nanoparticles.

315 As particle size will have an effect on antimicrobial activity, due to differences in
316 specific surface area, the samples are compared against each other in Table 2 keeping
317 an approximately constant mean particle size across all samples of approximately 200
318 nm (as performed for the zeta potentials presented in Fig. 5c. On this basis the Ag
319 nanoparticles showed significantly lower MIC and MBC values than Cu nanoparticles
320 towards both types of bacteria. Thus it can be surmised that Ag has a greater intrinsic
321 antimicrobial activity than Cu. The lowest MIC and MBC values were observed for
322 Ag/Cu nanoparticles in contact with both *B. subtilis* and *E. coli* either at the same
323 concentration of metal salts and chitosan or fixed nanoparticles size. Cu nanoparticles
324 displayed statistically the same antimicrobial effect as was obtained with a mixture of Ag
325 and Cu nanoparticles towards both *B. subtilis* and *E. coli*.

326 Bacteria bear a negative charge due to the excess number of carboxylic and
327 other groups which make the cell surface negative (Stoimenov, Klinger, Marchin, &
328 Klabunde, 2002). The nanoparticle suspensions produced here have positive charge as
329 revealed by zeta potential measurements. Electrostatic forces between positively
330 charged nanoparticles and negatively charged bacteria cells will enhance the effect of
331 antibacterial activity. Adhesion of nanoparticles to the surface of a bacterium alters its
332 membrane properties ultimately causing death (Li et al., 2008). The MIC and MBC of
333 the synthesized nanoparticles against both *B. subtilis* and *E. coli* revealed that the
334 Gram-positive bacteria were more susceptible than the Gram-negative bacteria to the
335 nanoparticles. This is most likely due to differences in bacterial cell-wall structure of
336 Gram-positive and Gram-negative with the Gram-negative cell wall having a structure
337 which is more complex than the Gram-positive cell wall.

338

339 **4. Conclusions**

340 Ag and Cu nanoparticles were synthesized using ascorbic acid as a reducing
341 agent in chitosan solutions using an efficient microwave heating method. Moreover, the

342 synthesis was fast, inexpensive, environmentally benign, energy efficient and does not
343 produce toxic waste. It was shown that nanoparticle size could be controlled by
344 manipulating the concentrations of chitosan and silver and copper nitrate used in their
345 synthesis. Particle size could be increased either by decreasing the chitosan
346 concentration or increasing the metal ion concentration. The nanoparticles produced
347 had a positive surface charge and the chitosan used in their synthesis contributed to the
348 stability of suspensions of such particles and prevented agglomeration. MIC and MBC
349 testing showed a potent bactericidal effect with Ag nanoparticles showing a greater
350 killing effect when compared to Cu nanoparticles at the same mean particle size. All the
351 nanoparticles showed very similar values for MIC and MBC which shows that the
352 nanoparticles have a bactericidal rather than bacteriostatic effect on these two bacteria.
353 The greatest antimicrobial effect was seen when Ag and Cu are combined during
354 synthesis to form alloyed particles. The use of the latter in medical applications is
355 currently being investigated.

356 **Acknowledgements**

357 NMZ thanks the Ministry of Education, Malaysia, University Malaysia Pahang and
358 Loughborough University for financial support. The authors would like to acknowledge
359 Mr David Smith for technical assistance with experiments.

360

361

362 **REFERENCES**

- 363 Ahmad, A., Mukherjee, P., Senapati, S., Mandal, D., Khan, M. I., Kumar, R., & Sastry,
364 M. (2003). Extracellular biosynthesis of silver nanoparticles using the fungus
365 *Fusarium oxysporum*. *Colloids and Surfaces B: Biointerfaces*, 28, 313–318.
- 366 Cao, X. L., Cheng, C., Ma, Y. L., & Zhao, C. S. (2010). Preparation of silver
367 nanoparticles with antimicrobial activities and the researches of their
368 biocompatibilities. *Journal of Materials Science: Materials in Medicine*, 21, 2861-
369 2868.
- 370 Dai, J. H., & Bruening, M. L. (2002). Catalytic nanoparticles formed by reduction of
371 metal ions in multilayered polyelectrolyte films. *Nano Letters*, 2(5), 497–501.
- 372 Datta, K. K. R., Kulkarni, C., & Eswaramoorthy, M. (2010). Aminoclay: A permselective
373 matrix to stabilize copper nanoparticles. *Chemical Communications (Cambridge,*
374 *England)*, 46, 616–618.
- 375 Díaz-Visurraga, J., Daza, Pozo Valenzuela, C., Becerra, García Cancino, A., & von
376 Plessing, C. (2012). Study on antibacterial alginate-stabilized copper nanoparticles
377 by FT-IR and 2D-IR correlation spectroscopy. *International Journal of*
378 *Nanomedicine*, 7, 3597-3612.
- 379 El-Nour, K. M. M. A., Eftaiha, A., Al-Warthan, A., & Ammar, R. A. A. (2010). Synthesis
380 and applications of silver nanoparticles. *Arabian Journal of Chemistry*, 3, 135–140.
- 381 Esumi, K., Takei, N., & Yoshimura, T. (2003). Antioxidant-potentiality of gold–chitosan
382 nanocomposites. *Colloids and Surfaces B: Biointerfaces*, 32, 117–123.
- 383 Flemming, C. A., & Trevors, J. T. (1989). Copper toxicity and chemistry in the
384 environment: A review. *Water, Air, and Soil Pollution*. 44, 143-158.
- 385 Hsiao, M.-T., Chen, S.-F., Shieh, D.-B., & Yeh, C.-S. (2006). One-pot synthesis of
386 hollow Au₃Cu₁ spherical-like and biomineral botallackite Cu₂(OH)₃Cl flowerlike

387 architectures exhibiting antimicrobial activity. *Journal of Physical Chemistry. B*, 110,
388 205–210.

389 Huang, H., Yuan, Q., & Yang, X. (2004). Preparation and characterization of metal–
390 chitosan nanocomposites. *Colloids and Surfaces B: Biointerfaces*, 39, 31–37.

391 Leung, T. C.-Y., Wong, C. K., & Xie, Y. (2010). Green synthesis of silver nanoparticles
392 using biopolymers, carboxymethylated-curdlan and fucoidan. *Materials Chemistry
393 and Physics*, 121, 402–405.

394 Li, Q., Mahendra, S., Lyon, D. Y., Brunet, L., Liga, M. V, Li, D., & Alvarez, P. J. J.
395 (2008). Antimicrobial nanomaterials for water disinfection and microbial control:
396 potential applications and implications. *Water Research*, 42, 4591–602.

397 Li, T, Albee, B., Alemayehu, M., Diaz, R., Ingham, L., Kamal, S., Rodriguez, M., &
398 Bishnoi, S.W. (2010). Comparative toxicity study of Ag, Au, and Ag-Au bimetallic
399 nanoparticles on *Daphnia magna*. *Analytical and Bioanalytical Chemistry*, 398, 689-
400 700.

401 Lim, S., & Hudson, S. M. (2004). Application of a fiber-reactive chitosan derivative to
402 cotton fabric as an antimicrobial textile finish. *Carbohydrate Polymers*, 56, 227–
403 234.

404 Mallick, K., Witcomb, M. J., & Scurrall, M. S. (2006). In situ synthesis of copper
405 nanoparticles and poly(o-toluidine): A metal–polymer composite material. *European
406 Polymer Journal*, 42, 670–675.

407 Marambio-Jones, C., & Hoek, E. M. V. (2010). A review of the antibacterial effects of
408 silver nanomaterials and potential implications for human health and the
409 environment. *Journal of Nanoparticle Research*, 12, 1531–1551.

410 Muzzarelli, R.A.A., Tanfani, F., & Emanuelli, M. (1984). Chelating derivatives of chitosan
411 obtained by reaction with ascorbic acid. *Carbohydrate Polymers*, 4, 137-151.

- 412 Muzzarelli, R.A.A. (1985). Removal of uranium from solutions and brines by a derivative
413 of ascorbic acid and chitosan. *Carbohydrate Polymers*, 5, 85-89 (1985).
- 414 Muzzarelli, R.A.A. (2010). Chitins and chitosans as immunoadjuvants and non-
415 allergenic drug carriers. *Marine Drugs*, 8, 292-312.
- 416 Muzzarelli, R.A.A. (2011) Potential of chitin/chitosan-bearing materials for uranium
417 recovery: An interdisciplinary review. *Carbohydrate Polymers*, 84, 54-63.
- 418 No, H. K., Park, N.Y., Lee, S.H., & Meyers, S. P. (2002). Antibacterial activity of
419 chitosans and chitosan oligomers with different molecular weights. *International*
420 *Journal of Food Microbiology*, 74, 65–72.
- 421 Perera, S., Bhushan, B., Bandara, R., Rajapakse, G., Rajapakse, S., & Bandara, C.
422 (2013). Morphological, antimicrobial, durability, and physical properties of untreated
423 and treated textiles using silver-nanoparticles. *Colloids and Surfaces A:*
424 *Physicochemical and Engineering Aspects*, 436, 975–989.
- 425 Ribeiro, S., Hussain, N., & Florence, A. T. (2005). Release of DNA from dendriplexes
426 encapsulated in PLGA nanoparticles. *International Journal of Pharmaceutics*, 298,
427 354–360.
- 428 Said-Galiev, E. E., Gamzazade, a. I., Grigor'ev, T. E., Khokhlov, a. R., Bakuleva, N. P.,
429 Lyutova, I. G., Shtykova, E. V., Dembo, K. A. & Volkov, V. V. (2011). Synthesis of
430 Ag and Cu-chitosan metal-polymer nanocomposites in supercritical carbon dioxide
431 medium and study of their structure and antimicrobial activity. *Nanotechnologies in*
432 *Russia*, 6, 341–352.
- 433 Sanpui, P., Murugadoss, A., Prasad, P. V. D., Ghosh, S. S., & Chattopadhyay, A.
434 (2008). The antibacterial properties of a novel chitosan–Ag-nanoparticle composite.
435 *International Journal of Food Microbiology*, 124, 142–146.

- 436 Sharma, V. K., Yngard, R. A., & Lin, Y. (2009). Silver nanoparticles: Green synthesis
437 and their antimicrobial activities. *Advances in Colloid and Interface Science*, *145*,
438 83–96.
- 439 Singare, D. S., Marella, S., Gowthamrajan, K., Kulkarni, G. T., Vooturi, R., & Rao, P. S.
440 (2010). Optimization of formulation and process variable of nanosuspension: An
441 industrial perspective. *International Journal of Pharmaceutics*, *402*, 213–220.
- 442 Solanki, J. N., Sengupta, R., & Murthy, Z. V. P. (2010). Synthesis of copper sulphide
443 and copper nanoparticles with microemulsion method. *Solid State Sciences*, *12*,
444 1560–1566.
- 445 Stoimenov, P. K., Klinger, R. L., Marchin, G. L., & Klabunde, K. J. (2002). Metal oxide
446 nanoparticles as bactericidal agents. *Langmuir*, *18*, 6679–6686.
- 447 Sundaresan, K., Sivakumar, A., Vigneswaran, C., & Ramachandran, T., . (2012).
448 Influence of nano titanium dioxide finish, prepared by sol-gel technique, on the
449 ultraviolet protection, antimicrobial, and self-cleaning characteristics of cotton
450 fabrics. *Journal of Industrial Textiles*, *41*, 259-277.
- 451 Taner, M., Sayar, N., Yulug, I. G., & Suzer, S. (2011). Synthesis, characterization and
452 antibacterial investigation of silver–copper nanoalloys. *Journal of Materials*
453 *Chemistry*, *21*, 13150-13154
- 454 Thakkar, K. N., Mhatre, S. S., & Parikh, R. Y. (2010). Biological synthesis of metallic
455 nanoparticles. *Nanomedicine: Nanotechnology, Biology, and Medicine*, *6*, 257–262.
- 456 Tolaymat, T. M., El Badawy, A. M., Genaidy, A., Scheckel, K. G., Luxton, T. P., &
457 Suidan, M. (2010). An evidence-based environmental perspective of manufactured
458 silver nanoparticle in syntheses and applications: A systematic review and critical
459 appraisal of peer-reviewed scientific papers. *Science of the Total Environment*,
460 *408*, 999–1006.

- 461 Twu, Y.-K., Chen, Y.-W., & Shih, C.-M. (2008). Preparation of silver nanoparticles using
462 chitosan suspensions. *Powder Technology*, 185, 251–257.
- 463 Valodkar, M., Modi, S., Pal, A., & Thakore, S. (2011). Synthesis and anti-bacterial
464 activity of Cu, Ag and Cu–Ag alloy nanoparticles: A green approach. *Materials*
465 *Research Bulletin*, 46, 384–389.
- 466 Wei, D., Sun, W., Qian, W., Ye, Y., & Ma, X. (2009). The synthesis of chitosan-based
467 silver nanoparticles and their antibacterial activity. *Carbohydrate Research*, 344,
468 2375–2382.
- 469 Xiong, J., Wu, X., & Xue, Q. (2013). Biomolecule-assisted synthesis of highly stable
470 dispersions of water-soluble copper nanoparticles. *Journal of Colloid and Interface*
471 *Science*, 1, 41-46.
- 472

473 **LIST OF FIGURES**

474

475 Figure 1. Nanoparticle suspensions of (a) Ag and (b) Cu synthesized in 10 mM metal
476 salts and different concentration of chitosan of 1, 2 and 3 % (w/v), respectively, (from
477 left to right) (c) From left to right: Ag, Cu, Ag + Cu and Ag/Cu nanoparticles suspensions
478 synthesized in 50 mM metal salts and 3 % (w/v) of chitosan.

479 Figure 2 Absorbance spectra of the nanoparticles of (a) Ag and (b) Cu synthesized in 10
480 mM metal salts and different concentrations of chitosan of 1, 2 and 3 % (w/v),
481 respectively, (c) Ag, Cu, Ag + Cu and Ag/Cu in 50 mM metal salts and 3 % (w/v) of
482 chitosan respectively.

483 Figure 3. Mean particle size of (a) Ag (b) Cu nanoparticles synthesized in 10 mM metal
484 salts and different concentrations of chitosan. Error bars represent standard deviations
485 from the mean in triplicate experiments. Different letters indicate differences significant
486 at $p \leq 0.05$.

487 Figure 4. Mean particle size of nanoparticles prepared by different concentrations of (a)
488 silver nitrate (b) copper nitrate (c) silver and copper nitrate (combined concentration) at
489 3 % (w/v) of chitosan. Error bars represent standard deviations from the mean of
490 triplicate experiments. Different letters indicate differences significant at $p \leq 0.05$.

491 Figure 5. Zeta potential of the nanoparticles of (a) Ag and Cu of 10 mM metal salts and
492 different concentration of chitosan (b) Ag, Cu, Ag + Cu and Ag/Cu of 50 mM metal salts
493 and 3% (w/v) of chitosan (c) Ag, Cu, Ag + Cu and Ag/Cu of with nitrate concentrations
494 adjusted to give 200 nm mean particle size (with 3% w/v chitosan). Error bars represent
495 standard deviation from the mean of triplicate experiments. Different letters indicate
496 differences significant at $p \leq 0.05$.

497

498 **LIST OF TABLES**

499 Table 1: MIC and MBC values of Ag, Cu, Ag/Cu and Ag + Cu nanoparticles synthesized
500 in 50 mM metal salts and 3% (w/v) of chitosan towards *B. subtilis* and *E. coli*. Identical
501 subscripted letters denote no statistically significant differences ($p>0.05$) between MIC
502 and MBC in column-based comparisons and identical superscripted letters denote no
503 statistically significant differences ($p>0.05$) in row-based comparisons as indicated by
504 one way ANOVA with Bonferroni multiple comparison tests.

505 Table 2: MIC and MBC values of Ag, Cu, Ag/Cu and Ag + Cu nanoparticles of 200 nm
506 mean particle size towards *B. subtilis* and *E. coli*. Identical subscripted letters denote no
507 statistically significant differences ($p>0.05$) between MIC and MBC in column-based
508 comparisons and identical superscripted letters denote no statistically significant
509 differences ($p>0.05$) in row-based comparisons as indicated by one way ANOVA with
510 Bonferroni multiple comparison tests.

511



(a)



(b)



(c)

Fig. 1.

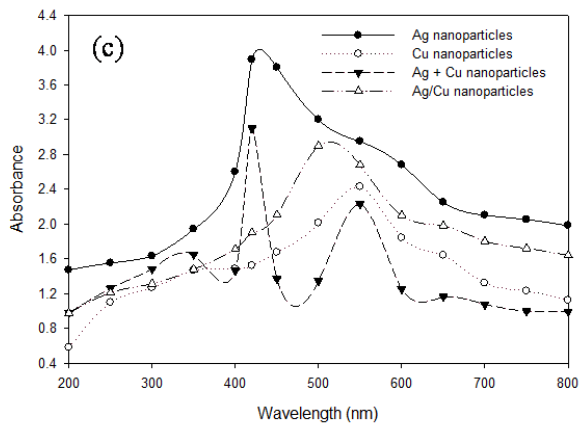
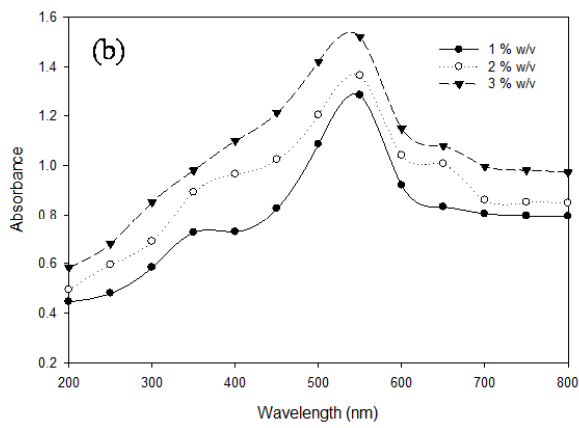
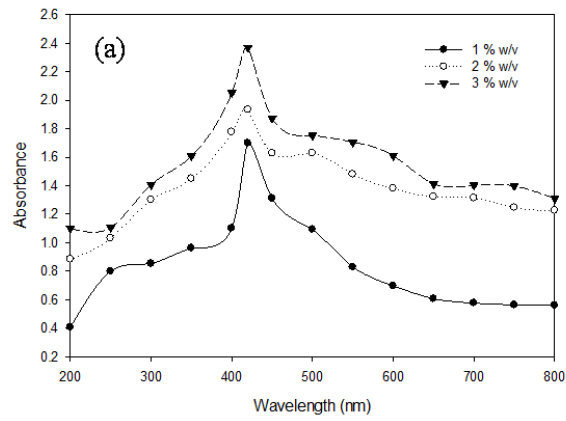
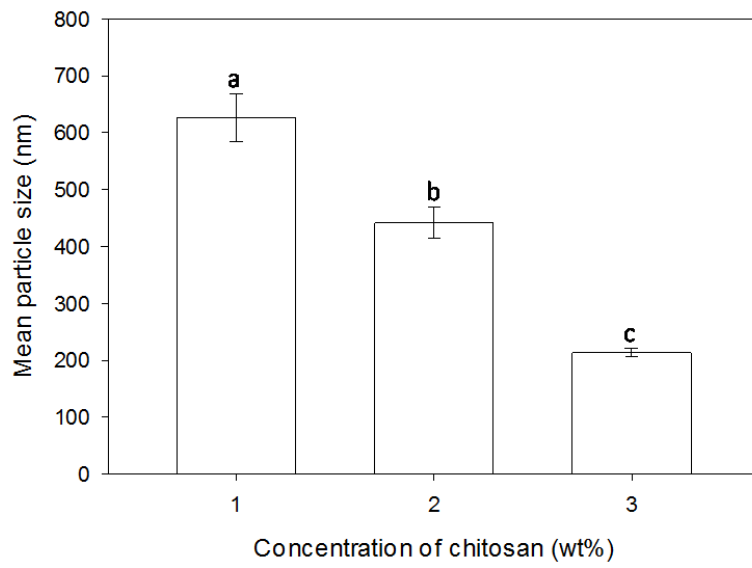
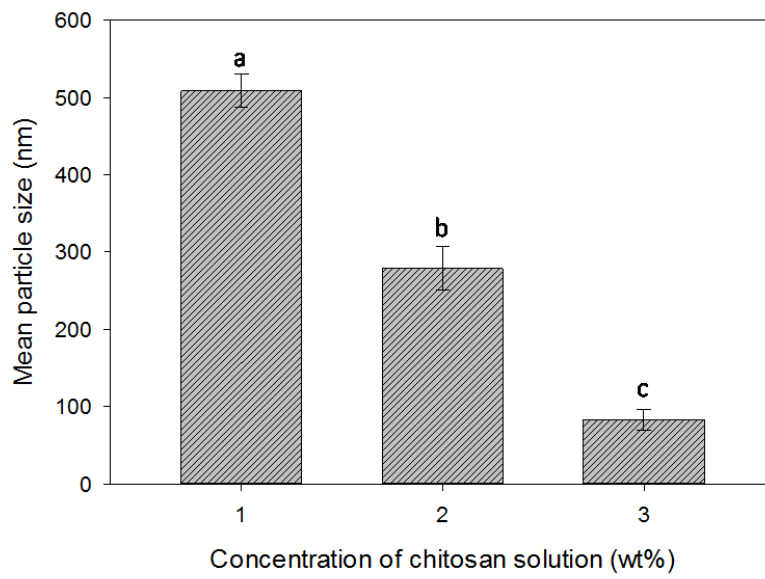


Fig. 2.



(a)



(b)

Fig. 3.

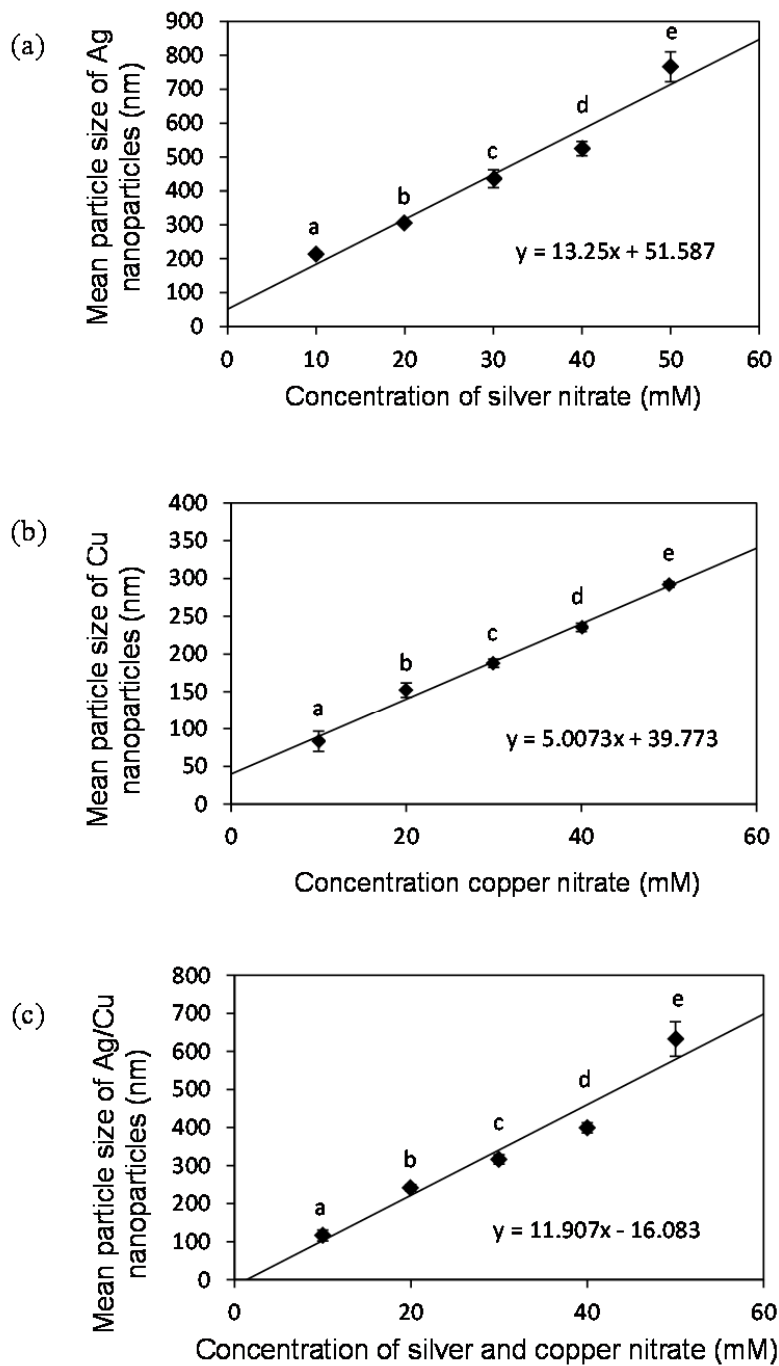


Fig. 4.

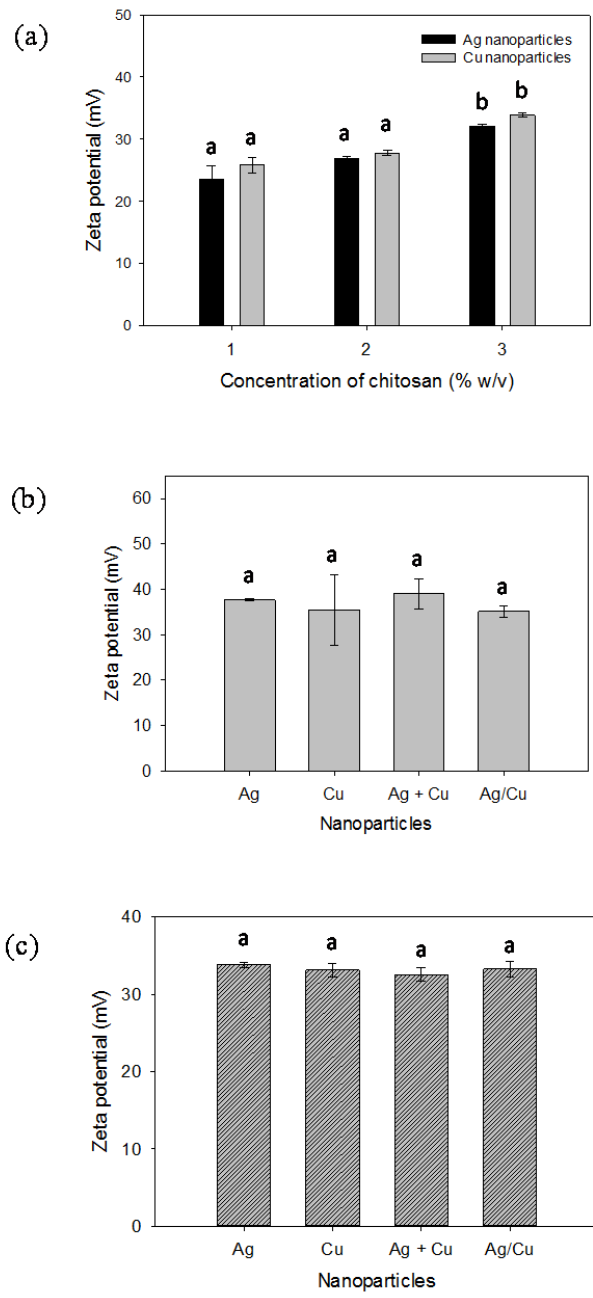


Fig. 5.

Table 1:

Bacteria	MIC (mg/L)				MBC (mg/L)			
	Ag	Cu	Ag+Cu	Ag/Cu	Ag	Cu	Ag+Cu	Ag/Cu
<i>B. subtilis</i>	0.652 ^A _a	0.313 ^B _a	0.576 ^A _a	0.179 ^C _a	0.666 ^A _a	0.438 ^B _a	0.596 ^A _a	0.194 ^C _a
<i>E.coli</i>	0.793 ^A _a	0.469 ^B _b	0.670 ^A _b	0.273 ^C _b	0.746 ^A _a	0.531 ^B _b	0.700 ^A _b	0.298 ^C _b

Table 2:

Bacteria	MIC (mg/L)				MBC (mg/L)			
	Ag	Cu	Ag+Cu	Ag/Cu	Ag	Cu	Ag+Cu	Ag/Cu
<i>B. subtilis</i>	0.172 ^A _a	0.320 ^B _a	0.262 ^B _a	0.054 ^C _a	0.189 ^A _a	0.387 ^B _a	0.336 ^B _a	0.061 ^C _a
<i>E.coli</i>	0.199 ^A _a	0.433 ^B _b	0.327 ^B _b	0.076 ^C _b	0.199 ^A _a	0.470 ^B _b	0.379 ^B _b	0.081 ^C _b